Journal of Solid State Chemistry **142,** 41–47 (1999)
Article ID jssc.1998.7981, available online at http://www.idealibrary.com on IDEAL®

Mechanically Activated Synthesis of Nanocrystalline Powders of Ferroelectric Bismuth Vanadate

K. Shantha, G. N. Subbanna, and K. B. R. Varma[1]

Materials Research Centre, Indian Institute of Science, Bangalore 560 012, India

Received March 16, 1998; in revised form July 28, 1998; accepted August 3, 1998

Mechanical milling of a stoichiometric mixture of Bi_2O_3 and V_2O_5 yielded nanosized powders of bismuth vanadate, $Bi_2VO_{5.5}$ (BiV). Structural evolution of the desired BiV phase, through an intermediate product ($BiVO_4$), was monitored by subjecting the powders, ball milled for various durations to X-ray powder diffraction (XRD), differential thermal analysis (DTA), and transmission electron microscopic (TEM) studies. XRD studies indicate that the relative amount of the BiV phase present in the ball-milled mixture increases with increase in milling time and its formation reaches completion within 54 h of milling. As-synthesized powders were found to stabilize in the high-temperature tetragonal (γ) phase. DTA analyses of the powders milled for various durations suggest that the BiV phase-formation temperature decreases with increase in milling time. The nanometric size (30 nm) of the crystallites in the final product was confirmed by TEM and XRD studies. TEM studies clearly demonstrate the growth of BiV on Bi_2O_3 crystallites. © 1999 Academic Press

1. INTRODUCTION

Nanocrystalline materials have immense potential for a variety of applications, by virtue of their improved electrical, magnetic, optical, and mechanical properties (1). They are attractive not only for their potential for technological applications, but also the feasibility which they provide to engineer their structures at atomic levels to generate solids with novel properties (2, 3). Among the various methods that are adopted to generate nanomaterials, mechanical alloying has been proved to be a very simple, effective, and economical technique for large scale production (4, 5). It has been successfully applied to enhance the kinetics of compound formation and phase transformations and also to synthesize novel materials (6), supersaturated solid solutions (7), and intermetallic compounds (8). The precise mechanism of mechanochemical synthesis varies depending on the specific system under investigation. However, the influence of mechanochemical activation on the kinetics of chemical reactions includes the reduction in the size of the particles and a consequent increase in the surface area. The formation of high defect density and the introduction of excess energy into the crystal lattice of the reactants, during intense grinding, enhance the diffusion rates.

Bismuth vanadate, $Bi_2VO_{5.5}$ (BiV) is a $n = 1$ member of the Aurivillius family of oxides which represents a technologically important class of electronic materials (9, 10). This compound is orthorhombic and ferroelectric at room temperature and undergoes two marked phase transitions at 725 and 835 K (11, 12). It is a good ionic conductor in its high temperature tetragonal (γ) phase (13). The use of BiV for a wide variety of applications such as catalysts (14), gas sensors (10), posistors (10), solid state electrolytes (15, 16), and positive electrode materials for lithium rechargeable batteries (17) has already been demonstrated. However, alternate synthetic methods need to be developed to realize the full potential of this material. It is known that high surface area thin films or powders are desirable for many industrial applications. There are reports on the synthesis of fine particle sized BiV powders by coprecipitation (18, 19) and sol–gel methods (20). We have made an attempt to synthesize nanocrystalline bismuth vanadate powders by mechanical activation. In this paper, the details regarding the synthesis of nano-BiV and the characterization of the powders using X-ray diffraction studies, differential thermal analysis, and electron microscopy are reported.

2. EXPERIMENTAL PROCEDURE

Commercial powders of Bi_2O_3 (>99.9% pure, Aldrich, with particle size 5 to 30 μm) and V_2O_5 (>99.9% pure, Aldrich, with particle size 1 to 15 μm), in a stoichiometric ratio, were mixed in acetone and put in an agate vial with an inner diameter of 6.5 cm and 16 agate balls of diameter 10 mm. The mixture was milled in a laboratory centrifugal ball mill (Fritsh, Pulverisette 6). Small amounts of the powder samples were taken out at regular intervals and were

[1] To whom correspondence should be addressed. Fax: 91-80-3341683. E-mail: kbrvarma@mrc.iisc.ernet.in.

0022-4596/99 $30.00

subjected to various analyses described below. The granulometric distribution of the initial and the milled powders was measured using a sizer (Malvern Instruments, Malvern, UK). The specific surface area measurements on the milled powders was done using the BET method (using Gemini 2375 V 3.02). The X-ray powder diffraction (XRD) analyses were done using a Scintag X-ray diffractometer (Cu$K\alpha$ radiation) at a slow scan of 1°/min. The variation in the crystallite size of one of the reactants Bi_2O_3 (V_2O_5 was not considered because the peak intensities corresponding to V_2O_5 are very small and hence the errors could be large) and the product BiV with milling time and the relative strain arising due to intense grinding were obtained from the broadening of X-ray peaks by adopting the Voigt single line approximation method (21). The most intense peaks of Bi_2O_3 and BiV were chosen for this purpose. In this method the integral breadths β (=area/peak intensity) and the full width at half maxima (w) were estimated for each peak and were corrected for instrumental contribution which was estimated by using a standard SiO_2 peak. The breadths of the Cauchy and the Gaussian components of the profile were separated by fitting the data into the emperical formulae given in Ref. (21). The crystallite size and the strain are given by the Cauchy and the Gaussian components, respectively. The annealing behavior of the powders was monitored using a Thermal analyzer STA 1500, Polymer Labs, at a heating rate of 20 K/min. Transmission electron microscopy (TEM) along with selected area electron diffraction (SAED) were conducted on the powder samples by employing a JEOL JEM 200 CX. Quantitative elemental analysis was done in a Laica S 360 SEM with LINK AN10000 energy dispersive X-ray analyzer (EDX) by employing ZAF-4 software.

3. RESULTS AND DISCUSSION

3.1. General

The milled powders were characterized by a fine and monodispersed granularity (Figs. 1a–1c). The mean diameter, $d(0.5)$, and the distribution in the particle diameter reduce significantly with increase in milling time. For instance, the particle size distribution recorded on the 16 h milled powder shows a sharp distribution peak centered around 1.5 μm, in contrast to a broad distribution peak obtained for 10 min milled powder. The powders milled for longer durations, i.e., more than 16 h (with finer particle sizes) could not be characterized because of the limitation associated with the instrument used.

The specific surface area analyses carried out on the milled powders suggest that the surface area of the powders increases from 0.9 m^2/g (10 min milled) to 9.8 m^2/g (54 h milled) on milling.

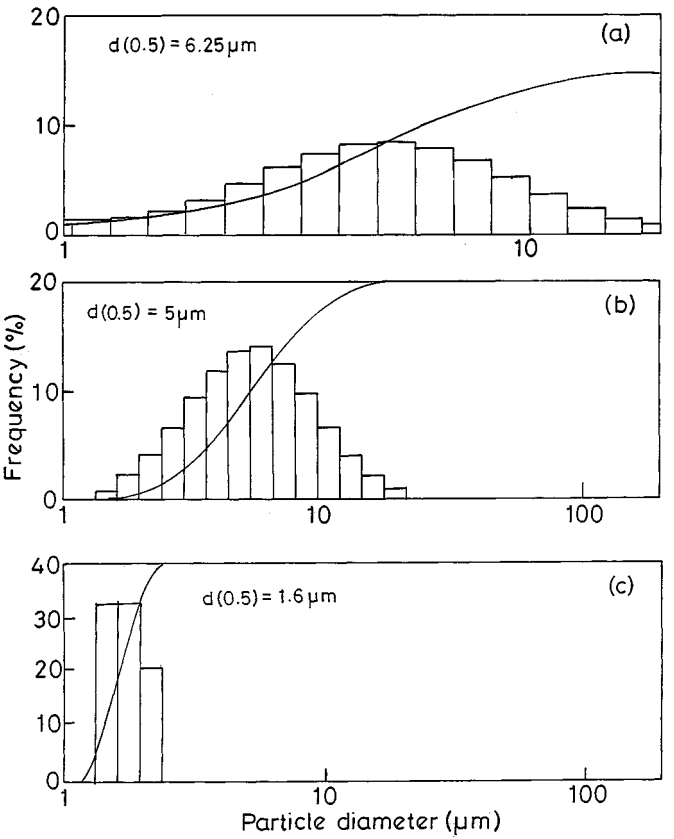

FIG. 1. Particle size distribution of powders milled for (a) 10 min, (b) 4 h, and (c) 16 h.

3.2. XRD Analysis

The evolution of the BiV phase was monitored by subjecting the powders milled for various durations to XRD studies. The XRD pattern recorded for 10 min milled sample (shown in Fig. 2a), indicates the presence of only the individual reactants Bi_2O_3 (marked B) and V_2O_5 (marked V). Figure 2b shows the XRD pattern obtained for the powders milled for 4 h. The peaks corresponding to $BiVO_4$ (marked BVO) could be identified in this pattern along with those of Bi_2O_3 and V_2O_5, suggesting the initiation of the reaction. This intermediate phase $BiVO_4$ evolves completely (Fig. 2c) by 16 h of milling. But on further ball milling, the formation of the desired BiV phase is evident (Fig. 2d) and the reaction is complete by 54 h. The corresponding XRD pattern, shown in Fig. 2e confirms the presence of only BiV peaks. The amount of BiV present in the mixture increases with increase in the milling time. Since we failed to notice the expected orthorhombic split even by slow scan, in the peaks corresponding to (0 2 0)–(6 0 0), (0 2 4)–(6 0 4), and (0 2 6)–(6 0 6), the present XRD pattern was indexed to a tetragonal cell with the lattice parameters $a = 3.9234$ Å and $c = 15.4925$ Å. These values are in good agreement with those reported for the high temperature γ-phase of BiV (13).

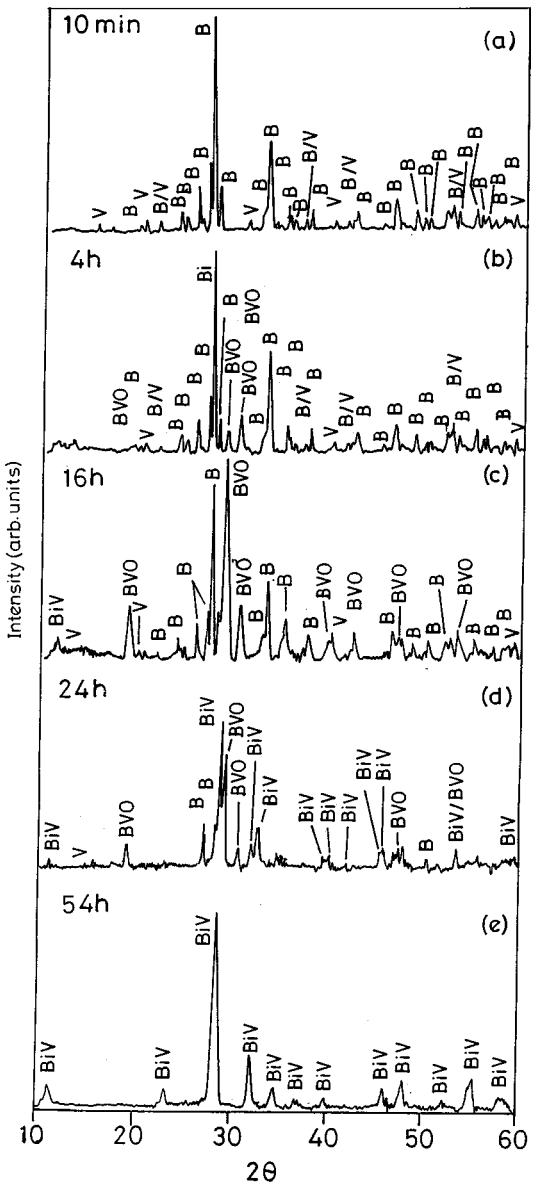

FIG. 2. XRD pattern recorded for the samples ball milled for (a) 10 min, (b) 4 h, (c) 16 h, (d) 24 h, and (e) 54 h. The peaks corresponding to Bi_2O_3, V_2O_5, $BiVO_4$, and $Bi_2VO_{5.5}$ are marked as B, V, BVO, and BiV, respectively.

Though the XRD result is convincing, there exists an element of uncertainty in concluding whether the sample has tetragonal or orthorhombic structure, because of the line broadening arising due to small crystallite size and nonuniform strain. To confirm the structure unambiguiously as carried out in the case of $BaTiO_3$ and PZT nanoparticles (22, 23), Raman spectroscopic studies have been taken up, the results of which will be communicated shortly. It is to be noted that the samples subjected to a small pressure (40 MPa) at room temperature or to heat treatment (770 K) attain the orthorhombic (α) phase of BiV. It implies that in small particles (as-prepared powders) the paraelectric tetragonal modification is energitically favored while the orthorhombic phase is more stable in larger particles. The stabilization of the paraelectric tetragonal phase in these nanosized particles of BiV, could be explained based on Gibbs–Thomson effect (24), according to which an additional hydrostatic pressure Δp ($\Delta p = \sigma/2r$, where r is the particle radius) could influence the interior of the small particles due to surface stresses σ. This additional stress acting on the atoms inside small particles can disturb the delicate balance that prevails between the short-range forces favoring the paraelectric tetragonal state and the long-range forces favoring the ferroelectric orthorhombic state and can eventually lead to the stabilization of the paraelectric state at room temperature. Stabilization of the tetragonal phase could also be explained in terms of the high surface energy of small particles. Fine particles because of their high specific surface area, possess excess surface energy as compared to bigger particles. This excess surface energy may contribute differentially to the relative free energies of orthorhombic and tetragonal structures and possibly lead to the room temperature stabilization of the tetragonal phase. As the particle size increases with increasing processing temperature or applied pressure, the internal pressure resulting from surface stresses fails to stabilize the tetragonal phase and the particles revert back to orthorhombic phase.

Based on the XRD analysis, we propose the following overall chemical reactions to represent the changes that were brought over by the milling process:

$$Bi_2O_3 + 0.5V_2O_5 \rightarrow BiVO_4 + 0.5Bi_2O_3$$

$$0.5Bi_2O_3 + BiVO_4 \rightarrow Bi_2VO_{5.5}(tetragonal).$$

The formation of intermediate products during mechanochemical activation is expected, as the change in the energy state of any of the reactants is possible during intense milling. This affects the equilibrium constants and hence allows the formation of compounds that do not form at the equilibrium state under ambient pressure and temperature. It is established that the nature and the relative amount of the intermediate compounds formed during chemical reactions do depend on the initial particle size of the reactants (25) and the rate of diffusion (26). In order to visualize the influence of the initial particle size on the BiV phase formation, we have subjected the stoichiometric mixture of Bi_2O_3 and V_2O_5 powders, with different particle sizes (average particle size ranging from 6.5 μm to few nanometers), obtained by ball milling for various durations, to heat treatment. It was observed that irrespective of the particle dimensions of the reactants involved, $BiVO_4$ phase always preceeds the formation of BiV. Reports on the preparation

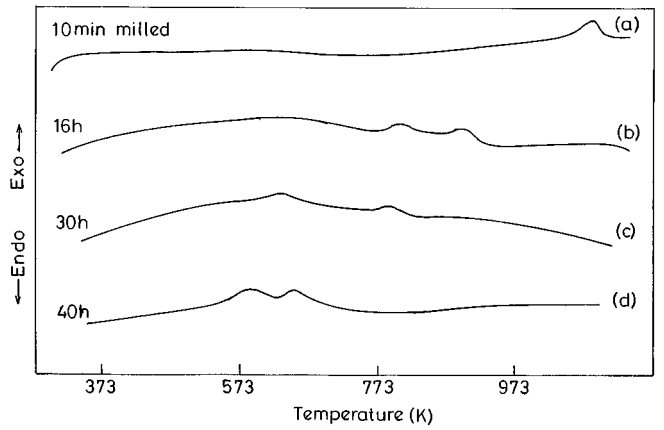

FIG. 3. Differential thermograms obtained on powders milled for various durations.

TABLE 1
Variation of Crystallite Size and the Associated Strain Estimated Based on XRD Data

Milling time (h)	Bi_2O_3 crystallite size (nm)	BiV crystallite size (nm)	Strain ($\times 10^{-3}$)
16	800	25	6
24	500	53	6.7
28	420	80	7.1
32	340	90	8.2
46	300	42	10.7
54	Absent	30	11

of BiV by sol–gel (20) and coprecipitation (18, 19) methods indicate that $BiVO_4$ is the intermediate phase even in these processes. Therefore, it is instructive to suggest that the activation barrier for the BiV nucleation is higher than that for $BiVO_4$.

The increase in peak broadening with increase in milling time (shown in Figs. 2a–e) indicates a reduction in the crystallite size. The peaks corresponding to the products ($BiVO_4$ or BiV) are broader than those corresponding to the reactants. The crystallite size and internal stress estimated based on X-ray peak broadening are given in Table 1. The Bi_2O_3 crystallite size decreases and the strain increases with increase in milling time. The EDX spectra recorded for the nanocrystalline BiV powder suggest the chemical composition to be that of BiV (Bi:V :: 2:1). However, the presence of a small amount of Si (<2 at.%) is detected, which could be arising from the agate vial and the balls.

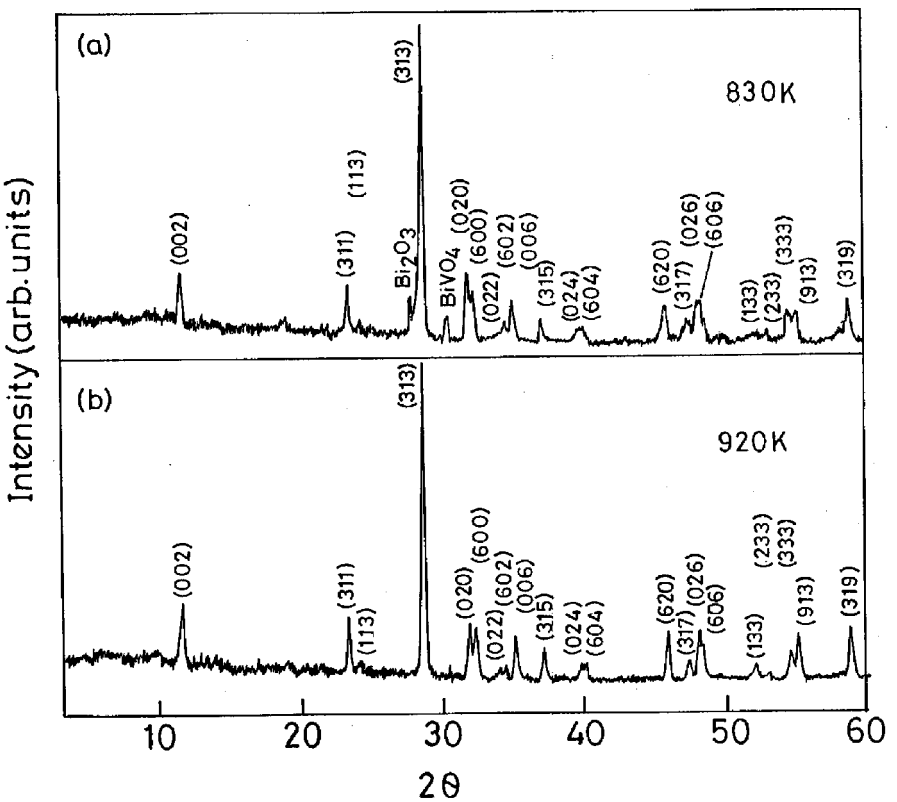

FIG. 4. XRD patterns of the powders retrieved from DTA at (a) 830 K and (b) 920 K.

3.3. *Differential Thermal Analysis*

Further investigations into the formation of BiV were carried out by means of differential thermal analysis (DTA). The differential thermograms corresponding to the powders milled for various durations are shown in Figs. 3a–3d. The powder ball milled for 10 min exhibits a single exotherm at 1077 K, whereas powders milled for longer durations are characterized by two broad exotherms. These exotherms shift to lower temperatures with increase in milling time (Figs. 3b–3d). In order to understand the origin of these exotherms, the samples ball milled for 16 h and subjected to DTA at various stages (830 K, prior to the second peak and 920 K, subsequent to the second peak) were analyzed by XRD. Figure 4(a and b) shows the X-ray patterns obtained for these samples. The X-ray peaks corresponding to the unreacted Bi_2O_3 and $BiVO_4$ could be identified along with those of BiV in the pattern shown in Fig. 4a. Therefore, the first exotherm in DTA could be attributed to the partial phase formation of BiV, whereas the X-ray pattern obtained for the sample heated to 920 K indicates the presence of only BiV peaks, which are sharp and distinct (Fig. 4b), implying

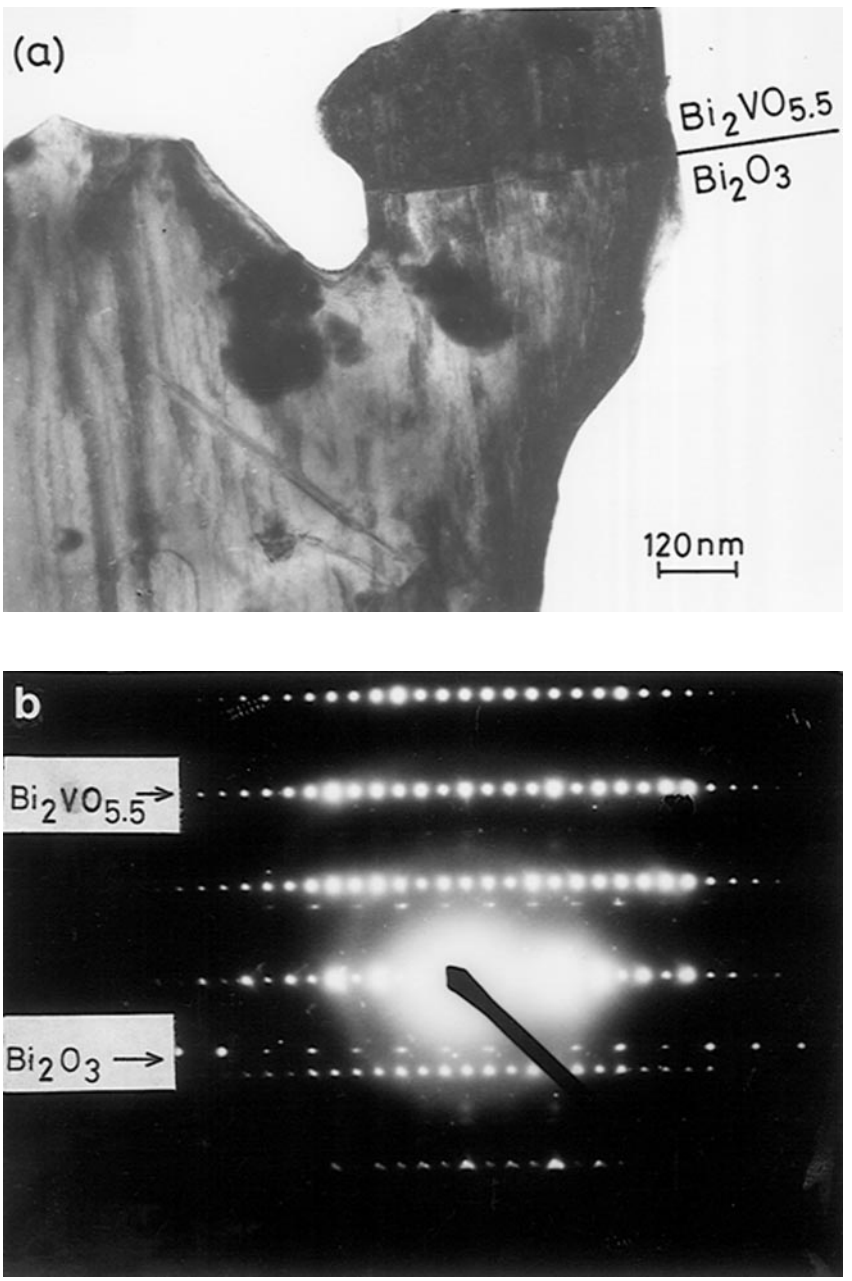

FIG. 5. (a) TEM image for 32-h milled powder indicating the growth of BiV on a Bi_2O_3 particle and (b) the corresponding SAED pattern.

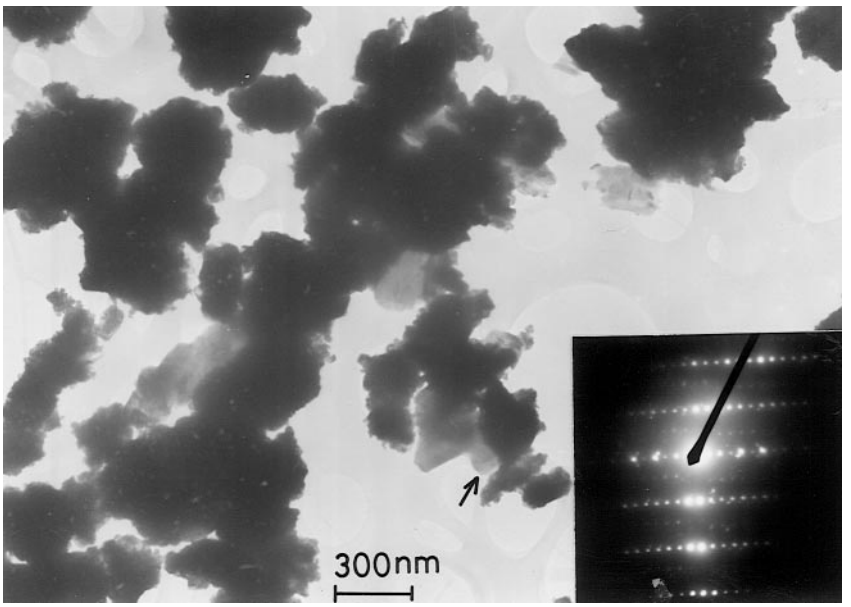

FIG. 6. TEM image recorded for the 54-h milled sample, showing a platymorphology. (Inset) Corresponding SAED pattern. The arrow marked indicates the particle on which the SAED pattern was recorded.

that the second exotherm is associated with the complete phase formation of BiV. Similar results were obtained on the 30- and 40-h milled powders.

3.4. Electron Microscopy

The powders at various stages of milling were characterized using TEM. The transmission electron micrograph obtained for the sample ball milled for 32 h is shown in Fig. 5a, wherein the evolution of BiV on a Bi_2O_3 particle is clearly seen. The corresponding electron diffraction image (Fig. 5b) shows a composite diffraction pattern of BiV and Bi_2O_3. This observation suggests that BiV growth takes place on Bi_2O_3 crystallites. The TEM and SAED analyses carried out on the samples ball milled upto 50 h indicate the presence of $BiVO_4$ phase along with Bi_2O_3 and BiV phases. The transmission electron micrograph of the powder, ball milled for 54 h, is shown in Fig. 6. The corresponding SAED image (shown as an inset) indicates the absence of $BiVO_4$ and Bi_2O_3 phases, confirming the complete formation of BiV. The sample ball milled for 54 h has a platymorphology, characteristic of the layered Aurivillius family of oxides. Since the powder is highly agglomerated, it is rather difficult to determine the grain size precisely by TEM studies.

4. CONCLUSION

In summary, nanosized powders of BiV (30 nm) have been prepared at room temperature via mechanical milling. The XRD studies carried out on the powders milled for various durations, confirm the evolution of the tetragonal BiV phase via an intermediate ferroelastic $BiVO_4$ phase. DTA analyses of the milled stoichiometric Bi_2O_3 and V_2O_5 powders indicated that the BiV phase formation temperature decreases with increase in milling time. The growth of BiV plates on the host Bi_2O_3 crystallites is confirmed by the electron diffraction studies. The characterization of the ceramics fabricated using these nanopowders for their dielectric, pyroelectric, and ferroelectric properties is in progress, the details of which will be communicated shortly.

ACKNOWLEDGMENT

One of the authors (K. Shantha), thanks CSIR, Government of India, for the financial support.

REFERENCES

1. H. Gleiter, *J. Appl. Crystallogr.* **24,** 79 (1991).
2. F. Cardellini, V. Contini, G. Mazzone, and A. Montone, *Phil. Mag. B* **76**(4), 629 (1997).
3. R. W. Seigel, *Sci. Am.* (Dec) 42 (1996).
4. E. Hellstern, H. J. Fecht, Z. Fu, and W. L. Johnson, *J. Appl. Phys.* **65**(1), 305 (1989).
5. Y. Chen, M. Marsh, J. S. Williams, and B. Ninham, *J. Alloys Compounds* **245,** 54 (1996).
6. P. Lacorre and R. Retoux, *J. Solid State Chem.* **132,** 443 (1997).
7. H. G. Jiang, R. J. Perez, M. L. Lau, and E. J. Lavernia, *J. Mater. Res.* **12**(6), 1429 (1997).
8. D. G. Morris and M. A. Morris, *Mater. Sci. Eng. A* **110,** 139 (1989).

9. A. A. Bush and Yu. N. Venevtsev, *Russ. J. Inorg. Chem.* **31**(5), 769 (1986).
10. P. B. Avakyan, M. D. Nersesyan, and A. G. Merzhanov, *Am. Ceram. Soc. Bull.* **75**(2), 50 (1996).
11. V. N. Borisov, Yu. M. Poplavko, P. B. Avakyan, and V. G. Osipian, *Sov. Phys. Solid State* **30**(5), 904 (1988).
12. K. B. R. Varma, G. N. Subbanna, T. N. Guru Row, and C. N. R. Rao, *J. Mater. Res.* **5,** 2718 (1990).
13. F. Abraham, J. C. Boivin, G. Mairresse, and G. Nawogrocki, *Solid State Ion.* **40/41,** 934 (1990).
14. A. Cherrak, R. Hubaut, Y. Barbaux, and G. Mairresse, *Catal. Lett.* **15,** 377 (1992).
15. P. Shuk, H.-D. Wiemhofer, U. Guth, W. Gopel, and M. Greenblatt, *Solid State Ion.* **89,** 179 (1996).
16. G. Mairesse, *in* "Fast Ion Transport in Solids" (B. Scrosati,Ed. p. 271. Kiuver, Amsterdam), 1993.
17. M. E. Arroyo y de Dompablo, F. Garcia-Alvarado, and E. Moran, *Solid State Ion.* **91,** 273 (1996).
18. K. V. R. Prasad, G. N. Subbanna, and K. B. R. Varma, *Bull. Mater. Sci.* **17**(1), 1 (1994).
19. A. K. Bhattacharya, K. K Mallick, and P. A. Thomas, *Solid State Commun.* **91**(5), 357 (1994).
20. J. W. Pell, J. Y. Ying, and H. C. zur Loye, *Mater. Lett.* **25,** 157 (1995).
21. Th. H. De Keijser, J. I. Langford, E. J. Mittemeijer, and A. B. P. Vogels, *J. Appl. Crystrallogr.* **15,** 308 (1982).
22. W. S. Cho, *J. Phys. Chem. Solids* **59,** 659 (1998).
23. J. F. Meng, R. S. Katiyar, G. T. Zou, and X. H. Wang, *Phys. Status Solidi A* **164,** 851 (1997).
24. G. Skandan, H. Hahn, and J. C. Parker, *Scr. Metall.* **25,** 2389 (1991).
25. W. Feitknecht, *Pure Appl. Chem.* **9,** 423 (1964).
26. L. K. Templeton and J. A. Pask, *J. Am. Ceram. Soc.* **42**(5), 212 (1959).